An FBG acoustic emission source locating system based on PHAT and GA*

SHEN Jing-shi (申景诗)[1,2], **ZENG Xiao-dong** (曾晓东)[1], **LI Wei** (李伟)[2]**, and **JIANG Ming-shun** (姜明顺)[3]

1. School of Physics and Optoelectronic Engineering, Xi'an Electronic and Science University, Xi'an 710071, China

2. Shandong Institute of Space Electronic Technology, Yantai 264000,China

3. School of Control Science and Engineering, Shandong University, Jinan 250061, China

(Received 13 June 2017; Revised 16 August 2017)

©Tianjin University of Technology and Springer-Verlag GmbH Germany 2017

Using the acoustic emission locating technology to monitor the health of the structure is important for ensuring the continuous and healthy operation of the complex engineering structures and large mechanical equipment. In this paper, four fiber Bragg grating (FBG) sensors are used to establish the sensor array to locate the acoustic emission source. Firstly, the nonlinear locating equations are established based on the principle of acoustic emission, and the solution of these equations is transformed into an optimization problem. Secondly, time difference extraction algorithm based on the phase transform (PHAT) weighted generalized cross correlation provides the necessary conditions for the accurate localization. Finally, the genetic algorithm (GA) is used to solve the optimization model. In this paper, twenty points are tested in the marble plate surface, and the results show that the absolute locating error is within the range of 10 mm, which proves the accuracy of this locating method.

Document code: A **Article ID:** 1673-1905(2017)05-0330-5

DOI https://doi.org/10.1007/s11801-017-7129-z

Acoustic emission is a phenomenon that the strain energy is released in the form of elastic waves which is caused by the deformation or rupture of the material or structure[1]. Acoustic emission detection technology can realize real-time monitoring of early damage of material or equipment[2]. Therefore, it has been widely used in many engineering fields, such as petrochemical, transportation, aerospace and material testing[3,4].

As one of the most important part of acoustic emission detection, acoustic emission localization technique can be used to locate the acoustic emission source[5]. Acoustic emission signal is a kind of non-stationary random signal, which is very complex. It needs to extract the effective information of acoustic emission signal by using the signal processing technology[6-8]. The selections of the acoustic emission sensors and the algorithm are two keys of the acoustic emission locating technology. In recent years, the fiber Bragg grating (FBG) sensor[9-13] has been used in the research of acoustic emission locating technology. For the selection of the acoustic emission locating algorithm, the time difference location algorithm is widely used, but the time difference is difficult to be determined, and the positioning accuracy is also affected by signal attenuation[14-16]. For the extraction of the time difference, Jin et al[17] used the generalized cross correlation method to extract the time difference. Huang et al[18] deduced time delay of acoustic emission signal through the phase difference obtained by combining wavelet decomposition and all phase frequency analyses.

In order to obtain the accurate localization results, the acoustic emission source must be ensured in the geometrical pattern formed by the sensor array. When the acoustic emission source is out of the geometrical pattern, the measurement results will have a large error. However, in many cases, due to hard judgment of the acoustic emission source, you cannot accurately estimate the possible area of acoustic emission source, which brings some difficulties for acoustic emission locating. Therefore, aiming at the above shortcomings, this paper presents an acoustic emission source location method based on optimization method, which does not need to know the wave velocity in advance, and has higher accuracy for both inner and outer of the location array.

The principle of acoustic emission source localization based on the optimization method is illustrated by the method of triangle array location as shown in Fig.1.

In Fig.1, $P(x_0, y_0)$ is the location of acoustic emission source, and $S_i(x_i, y_i)$ is the location of acoustic emission sensor. d_i and t_i are the distance and arrive time between P and S_i, which can be expressed as

* This work has been supported by the National Natural Science Foundation of China (No.41472260), the Fundamental Research Funds of Shandong University (No.2016JC012), and the Young Scholars Program of Shandong University (No.2016WLJH30).

** E-mail: sduliwei2017@163.com

$$d_i = \sqrt{(x_i - x_0)^2 + (y_i - y_0)^2}\,, \tag{1}$$

$$t_i = \frac{d_i}{c} = \frac{\sqrt{(x_i - x_0)^2 + (y_i - y_0)^2}}{c}\,. \tag{2}$$

For eliminating c, the ratio analysis equations can be obtained as

$$\frac{d_2}{d_1} = \frac{t_2}{t_1} = \frac{\sqrt{(x_2 - x_0)^2 + (y_2 - y_0)^2}}{\sqrt{(x_1 - x_0)^2 + (y_1 - y_0)^2}} = r_{21}\,, \tag{3}$$

$$\frac{d_3}{d_1} = \frac{t_3}{t_1} = \frac{\sqrt{(x_3 - x_0)^2 + (y_3 - y_0)^2}}{\sqrt{(x_1 - x_0)^2 + (y_1 - y_0)^2}} = r_{31}\,. \tag{4}$$

Eqs.(3) and (4) can form a set of equations as

$$\begin{cases} \dfrac{t_2}{t_1} = \dfrac{\sqrt{(x_2 - x_0)^2 + (y_2 - y_0)^2}}{\sqrt{(x_1 - x_0)^2 + (y_1 - y_0)^2}} \\ \dfrac{t_3}{t_1} = \dfrac{\sqrt{(x_3 - x_0)^2 + (y_3 - y_0)^2}}{\sqrt{(x_1 - x_0)^2 + (y_1 - y_0)^2}} \end{cases}. \tag{5}$$

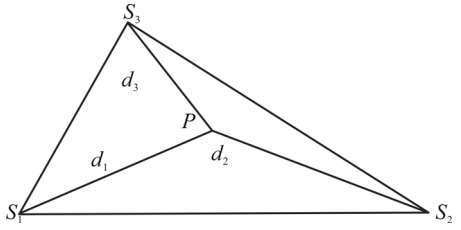

Fig.1 The principle of triangle array location method

Therefore, by solving Eq.(5), the positioning of the acoustic emission source can be achieved. The sum of the squares of Eqs.(3) and (4) can be expressed as

$$r_{21}^2 + r_{31}^2 = \left(\frac{d_2}{d_1}\right)^2 + \left(\frac{d_3}{d_1}\right)^2 = \left(\frac{t_2}{t_1}\right)^2 + \left(\frac{t_3}{t_1}\right)^2 = \frac{(x_2 - x_0)^2 + (y_2 - y_0)^2 + (x_3 - x_0)^2 + (y_3 - y_0)^2}{(x_1 - x_0)^2 + (y_1 - y_0)}\,. \tag{6}$$

Using $P'(x, y)$ instead of $P(x_0, y_0)$, the error function $E(x, y)$ can be defined as

$$E(x,y) = \left\{(x_2 - x)^2 + (y_2 - y)^2 + (x_3 - x)^2 + (y_3 - y)^2 - (r_{21}^2 + r_{31}^2)\left[(x_1 - x)^2 + (y_1 - y)^2\right]\right\}^2. \tag{7}$$

The minimum value of $E(x, y)$ is the acoustic emission source of $P(x_0, y_0)$. Thus the solution of Eq.(5) is changed to an optimization problem:

$$\begin{cases} \min \quad f(x,y) = E(x,y) \\ s.t. \quad x_{\min} < x < x_{\max} \\ \qquad y_{\min} < y < y_{\max} \end{cases}. \tag{8}$$

Define t_{ij} is time difference between S_i and S_j, i.e.,

$$t_{ij} = t_i - t_j\,. \tag{9}$$

Then, according to Eqs.(2) and (9), we can get the following equation:

$$\frac{t_{21}}{t_{31}} = \frac{\sqrt{(x_2 - x)^2 + (y_2 - y)^2} - \sqrt{(x_1 - x)^2 + (y_1 - y)^2}}{\sqrt{(x_3 - x)^2 + (y_3 - y)^2} - \sqrt{(x_1 - x)^2 + (y_1 - y)^2}}\,. \tag{10}$$

Substituting Eq.(10) into $E(x, y)$, it can be obtained that

$$E(x,y) = \left(\frac{\sqrt{(x_2 - x)^2 + (y_2 - y)^2} - \sqrt{(x_1 - x)^2 + (y_1 - y)^2}}{\sqrt{(x_3 - x)^2 + (y_3 - y)^2} - \sqrt{(x_1 - x)^2 + (y_1 - y)^2}} - \frac{t_{21}}{t_{31}}\right)^2. \tag{11}$$

To obtain the position of the acoustic emission source accurately, the expression of $E(x, y)$ is modified as

$$\begin{aligned} E(x,y) = {} & \left\{t_{23}\left[\sqrt{(x_1 - x)^2 + (y_1 - y)^2} - \sqrt{(x_2 - x)^2 + (y_2 - y)^2}\right] - t_{12}\left[\sqrt{(x_2 - x)^2 + (y_2 - y)^2} - \sqrt{(x_3 - x)^2 + (y_3 - y)^2}\right]\right\}^2 + \\ & \left\{t_{31}\left[\sqrt{(x_2 - x)^2 + (y_2 - y)^2} - \sqrt{(x_3 - x)^2 + (y_3 - y)^2}\right] - t_{23}\left[\sqrt{(x_3 - x)^2 + (y_3 - y)^2} - \sqrt{(x_1 - x)^2 + (y_1 - y)^2}\right]\right\}^2 + \\ & \left\{t_{12}\left[\sqrt{(x_3 - x)^2 + (y_3 - y)^2} - \sqrt{(x_1 - x)^2 + (y_1 - y)^2}\right] - t_{31}\left[\sqrt{(x_1 - x)^2 + (y_1 - y)^2} - \sqrt{(x_2 - x)^2 + (y_2 - y)^2}\right]\right\}^2 = \\ & \left[t_{23}(d_1 - d_2) - t_{12}(d_2 - d_1)\right]^2 + \left[t_{31}(d_2 - d_3) - t_{23}(d_3 - d_1)\right]^2 + \\ & \left[t_{12}(d_3 - d_1) - t_{31}(d_1 - d_2)\right]^2. \end{aligned} \tag{12}$$

In this way, by using some optimization algorithms, the value of $E(x, y)$ can be minimized and the position (x_0, y_0) can be got.

However, due to $t_{31}=t_{12}+t_{23}$, when using t_{ij} instead of t_i in Eq.(5), we can only get two time differences t_{ij}. To obtain the unique solution of Eq.(5), a set of independent time difference must be added. Therefore, when using this locating method, at least four sensors are required. Thus, when using four sensors, $E(x, y)$ can be expressed based on the above method as

$$\begin{aligned} E(x,y) = {} & \left[t_{12}(d_2 - d_3) - t_{23}(d_1 - d_2)\right]^2 + \left[t_{12}(d_3 - d_4) - t_{34}(d_1 - d_2)\right]^2 + \\ & \left[t_{12}(d_4 - d_1) - t_{41}(d_1 - d_2)\right]^2 + \left[t_{12}(d_2 - d_4) - t_{24}(d_1 - d_2)\right]^2 + \\ & \left[t_{12}(d_1 - d_3) - t_{13}(d_1 - d_2)\right]^2 + \left[t_{23}(d_3 - d_4) - t_{34}(d_2 - d_3)\right]^2 + \\ & \left[t_{23}(d_4 - d_1) - t_{41}(d_2 - d_3)\right]^2 + \left[t_{23}(d_2 - d_4) - t_{24}(d_2 - d_3)\right]^2 + \\ & \left[t_{23}(d_1 - d_3) - t_{13}(d_2 - d_3)\right]^2 + \left[t_{34}(d_4 - d_1) - t_{41}(d_3 - d_4)\right]^2 + \\ & \left[t_{34}(d_2 - d_3) - t_{23}(d_3 - d_4)\right]^2 + \left[t_{34}(d_1 - d_3) - t_{13}(d_3 - d_4)\right]^2 + \\ & \left[t_{41}(d_2 - d_4) - t_{24}(d_4 - d_1)\right]^2 + \left[t_{41}(d_1 - d_3) - t_{13}(d_4 - d_1)\right]^2 + \\ & \left[t_{24}(d_1 - d_3) - t_{13}(d_2 - d_4)\right]^2, \end{aligned} \tag{13}$$

where $d_i = \sqrt{(x_i - x)^2 + (y_i - y)^2}$ with i=1,2,3,4.

In Eq.(13), t_{ij} and t_{kl} are time differences of arrival of different sensor groups for acoustic emission signals. To obtain accurate source coordinates, the time difference

value must be obtained.

Assuming two acoustic emission sensors at different positions, the signal $x_1(n)$ and $x_2(n)$ received from the same source are respectively defined as

$$x_1(n) = s(n-\tau_1) + n_1(n), \tag{14}$$

$$x_2(n) = s(n-\tau_2) + n_2(n), \tag{15}$$

where $s(n)$ is acoustic emission signal, and $n_1(n)$ and $n_2(n)$ are noises.

The cross correlation function of $x_1(n)$ and $x_2(n)$ is

$$R_{12}(\tau) = E\left[x_1(n)x_2(n-\tau)\right]. \tag{16}$$

As shown in Fig.2, H_1 and H_2 are filtering functions, the signal noise is removed. So it can be expressed as

$$R_{12}(\tau) = E\left[x_1(n)x_2(n-\tau)\right] = \int_0^{\pi} G_{12}(\omega)\mathrm{e}^{\mathrm{j}\omega\tau}\mathrm{d}\omega, \tag{17}$$

where $G_{12}(\omega)$ is the cross power spectral function $x_1(n)$ and $x_2(n)$.

After filtering $x_1(n)$ and $x_2(n)$, $G_{12}(\omega)$ can be written as

$$G_{g12}(\omega) = H_1(\omega)H_2^*(\omega)G_{12}(\omega), \tag{18}$$

where $H_2^*(\omega)$ is complex conjugate of $H_2(\omega)$. Therefore, the generalized cross correlation function of $x_1(n)$ and $x_2(n)$ can be expressed as

$$R_{g12}^{(g)}(\tau) = \int_0^{\pi} \psi_g(\omega)G_{12}(\omega)\mathrm{e}^{\mathrm{j}\omega\tau}\mathrm{d}\omega, \tag{19}$$

where $\psi_g(\omega) = H_1(\omega)H_2^*(\omega)$ is the generalized frequency domain weight component. In this paper, phase transform (PHAT) is chosen as the weighted function, so $\psi_g(\omega)$ is written as

$$\psi_g(\omega) = \frac{1}{\left|G_{12}(\omega)\right|}. \tag{20}$$

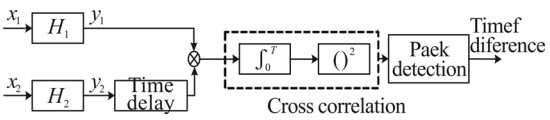

Fig.2 The block diagram of the time delay estimation using noise removal

Compared with the traditional optimal methods, genetic algorithm is selected to solve the acoustic emission source location equations.

(1) Problem description

The objective function $E(x, y)$ of acoustic emission source locating problem is shown in Eq.(13). In this paper, acoustic emission source locating experiments were carried out on the marble plate with size of 800 mm×800 mm×5 mm. Therefore, the range of decision variables of x and y is (0 m, 0.8 m).

(2) Encoding method

In this paper, we use a 10 bit binary string to represent the decision variables of x and y. Therefore, the calculation accuracy will reach 0.8/1 023≈0.78 mm. A chromosome is obtained by combining the binary strings of two decision variables together to form a binary string with 20 bits, and a chromosome is obtained as shown in Fig.3.

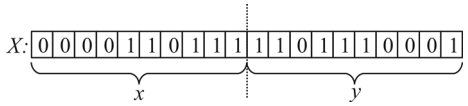

Fig.3 Schematic diagram of a chromosome

(3) Decoding method

In the process of decoding, a binary string with length of 20 bits is divided into two binary strings from the middle. And then these two binary strings are converted to the corresponding decimal integers of m and n. Finally, the decimal integer is converted to the actual value of the domain by

$$\begin{cases} x = \dfrac{0.8}{1\,023}\cdot m \\ y = \dfrac{0.8}{1\,023}\cdot n \end{cases}. \tag{21}$$

(4) Individual evaluation method

The adaptation of the individual is defined as

$$F(X) = \begin{cases} C_{\max} - f(X), & \text{if } f(X) < C_{\max} \\ 0, & \text{if } f(X) \geq C_{\max} \end{cases}, \tag{22}$$

where $C_{\max}$ is a preset appropriate larger constant.

(5) Design genetic operator

The choice of the selection operator is based on the classical wheel roulette. Crossover operator is realized by using single point crossover. The mutation operator is implemented by the basic bit mutation method.

(6) Determining the algorithm parameters

In this algorithm, the parameters are set as group size of M=40, maximum iteration number of T=100, crossover probability of p_c=0.7 and variation probability of p_m=0.05.

At this point, the genetic algorithm is constructed to solve the problem of the acoustic emission source location. The basic steps of the algorithm are shown in Fig.4.

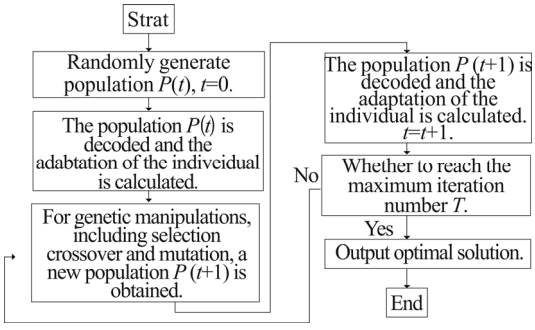

Fig.4 Genetic algorithm solving flow chart

In a Bragg grating, the wavelength of the reflection peak is

$$\lambda_B = 2n\Lambda, \tag{23}$$

where λ_B is called Bragg wavelength, n is FBG effective refractive index, and Λ is grating period. Merely

considering the influence of strain, we can get

$$\frac{\Delta\lambda_B}{\lambda_B}=(1-P_e)\cdot\varepsilon, \tag{24}$$

where $\Delta\lambda_B$ is the FBG wavelength changes, P_e is effective light function and ε is strain.

As shown in Fig.5, the acoustic emission locating system is constructed, and the acoustic emission signals are produced by breaking lead. The light emitted from the laser passes through the isolator and coupler into the fiber grating sensor, and the intensity change of the reflected light of the sensor is related to the frequency of the acoustic wave. The reflected light enters the photoelectric conversion circuit through the coupler and converts into an electric signal to realize the measurement of the acoustic emission signal. The selected laser type is Santec TSL-510, and the spectral bandwidth of the output is less than 0.1 pm.

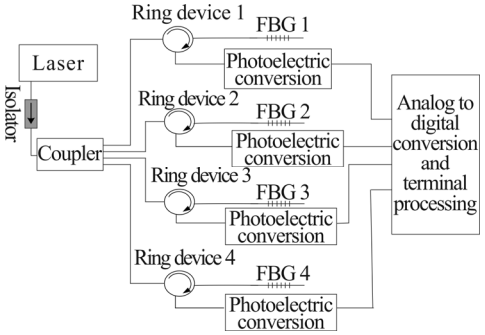

Fig.5 Schematic diagram of acoustic emission locating system

Four FBG acoustic emission sensors are exposed to the marble plate surface. The concrete parameters of FBG1, FBG2, FBG3 and FBG4 are as follows: central wavelengths of FBG1, FBG2, FBG3 and FBG4 are 1 565.260 nm, 1 565.255 nm, 1 565.240 nm and 1 565.250 nm, 3 dB bandwidth is 0.25 nm, the grating length is 10 mm, and the reflectivity is more than 90%. Tunable narrow band laser wavelength is 1 565.280 nm, and power is 5 mV. Four sensors are arranged as shown in Fig.6.

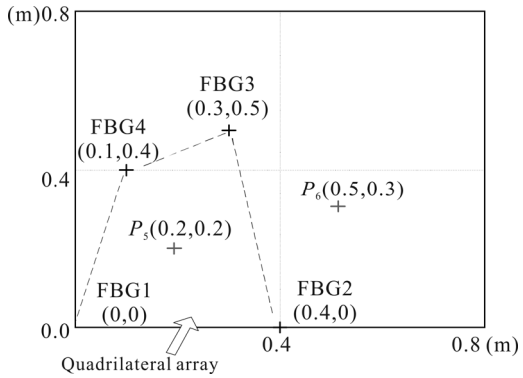

Fig.6 Layout of four sensors

The locating analysis is carried out in the inner and outer sides of the quadrilateral.

First, the acoustic emission locating is carried out in the inner point P_5(0.20 m, 0.20 m) of the quadrilateral by the simulation of the lead. Take t_{23} as an example, and the time difference is extracted. The signal detected by FBG2 and FBG3 is shown in Fig.7. According to Fig.7, PHAT weighted generalized cross correlation time difference estimation algorithm are conducted, and $t_{23}=-1.00\times10^{-5}$ s.

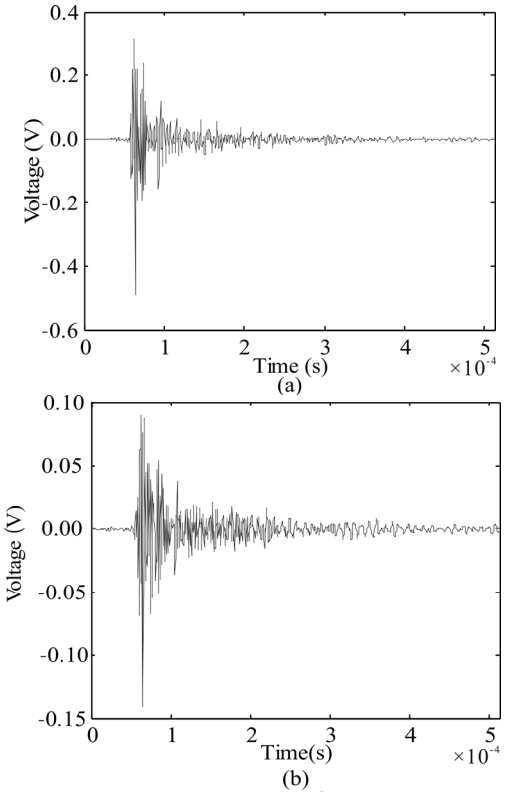

Fig.7 Signal detected by (a) FBG2 and (b) FBG3

Based on the above progress, another five sets of time difference are obtained as $t_{12}=0$ s, $t_{34}=1.75\times10^{-5}$ s, $t_{41}=-1.70\times10^{-5}$ s, $t_{24}=1.80\times10^{-5}$ s and $t_{13}=-1.00\times10^{-5}$ s.

Genetic algorithm is used to solve the problem, and the iterative process is shown in Fig.8.

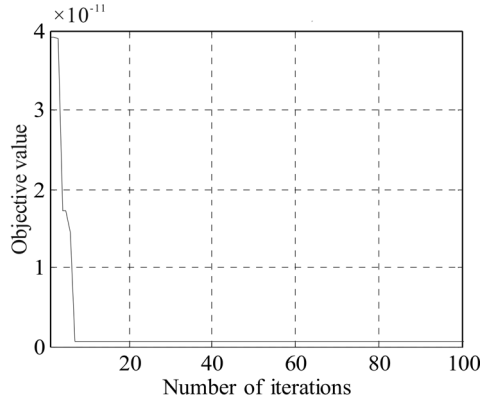

Fig.8 Genetic algorithm solving curve for the experiment with P_5(0.20 m, 0.20 m)

Then, based on the same progress of the above experiment, another experiment is carried out in the outer

point P_6(0.50 m, 0.30 m) of the quadrilateral by the simulation of the lead. Totally, six sets of time difference are obtained by using PHAT weighted generalized cross correlation time difference estimation algorithm, which are $t_{12}=7.90\times10^{-5}$ s, $t_{23}=1.00\times10^{-5}$ s, $t_{34}=-3.95\times10^{-5}$ s, $t_{41}=-5.10\times10^{-5}$ s, $t_{24}=-2.80\times10^{-5}$ s and $t_{13}=8.95\times10^{-5}$ s.

Genetic algorithm is used to solve the problem, and the iterative process is shown in Fig.9.

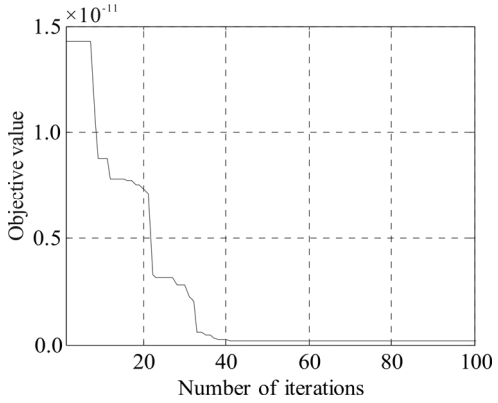

Fig.9 Genetic algorithm solving curve for the experiment with P_6(0.50 m, 0.30 m)

In the location experiment, ten points are carried out in the inner of the quadrilateral, and another ten points are carried out in the outer. The predicted results and actual location of these 20 test points are shown in Tab.1, and the absolute error of locating e is calculated by

$$e=\sqrt{(x_{\mathrm{p}}-x_{\mathrm{a}})^2+(y_{\mathrm{p}}-y_{\mathrm{a}})^2}\ , \tag{25}$$

where x_{p} and y_{p} are the predicted results, and x_{a} and y_{a} are the actual locations.

Tab.1 The predicted locating results, the actual location results and the absolute error (mm)

N	$(x_{\mathrm{a}}, y_{\mathrm{a}})$	$(x_{\mathrm{p}}, y_{\mathrm{p}})$	e
1	(100, 100)	(97.2,98.6)	3.13
2	(100, 200)	(98.4, 196.5)	3.4
3	(100, 300)	(96.3, 298.3)	4.07
4	(200, 100)	(204.7, 98.1)	5.07
5	(200, 200)	(198.6, 203.5)	3.76
6	(200, 300)	(195.2, 294.1)	7.6
7	(200, 400)	(201.4, 400.8)	1.6
8	(300, 100)	(294.8, 98.9)	5.31
9	(300, 200)	(300, 195.6)	4.4
10	(300, 300)	(301.6, 305.7)	5.92
11	(400, 200)	(404.6, 205.6)	7.25
12	(400, 300)	(398.4, 305.2)	5.44
13	(400, 400)	(402.5, 406.3)	6.78
14	(500, 300)	(504, 297.6)	8.59
15	(500, 400)	(498.1, 395.7)	4.7
16	(100, 500)	(98, 503)	3.6
17	(100, 600)	(96.5, 602.4)	4.24
18	(200, 500)	(194.6, 497.3)	6.04
19	(300, 600)	(298, 596.4)	4.12
20	(400, 600)	(403.1, 594.2)	6.58

From the experimental results, we can get that the absolute acoustic emission source locating error is within the range of 10 mm by using the optimization method and the PHAT weighted generalized cross correlation algorithm. And the sensor can be placed arbitrarily. Regardless of the acoustic emission source locating in the inner or outer sides of the quadrilateral, locating results are quite accurate.

References

[1] R. Ernst and F. Zwimpfer, J. Dual. Ultrasonics **64**, 139 (2016).

[2] N Zhao and KQ Ding, Applied Mechanics and Materials **330**, 396 (2013).

[3] Wang Q, Gao S H, Zhu L, Zou B and Jiang S X, Safety Health & Environment **16**, 37 (2016). (in Chinese)

[4] Zhang H F, Chen X, Ma B L, Li Z L, Zhang H D and Liu Z C, Automation in Petro-Chemical Industry **51**, 53 (2015).(in chinese)

[5] T. Kundu, Ultrasonics **54**, 25 (2014).

[6] Y. Kang, W. Zhu, G. Chen and X. Yin, Rock and Soil Mechanics **32**, 2079 (2011).

[7] Z. Zheng, J. Hua, B. Jiang, W. Lu, H. Wen and X. Yu, Chinese Journal of Sensors and Actuators **26**, 722 (2013).

[8] Y. Shan, P. Sun, Y. Xu, H. Fu and S. Xie, Chinese Journal of Sensors and Actuators **26**, 402 (2013).

[9] T. Osuch, P. Gąsior, K. Markowski and K. Jędrzejewski., Bulletin of the Polish Academy of Sciences Technical Sciences **62**, 627 (2014).

[10] J. Lu, B. Wang and D. Liang, Applied Optics **52**, 2346 (2013).

[11] Y. Zhang, C. Zhao and J. Chen, Chinese Journal of Quantum Electronics **30**, 608,(2013).

[12] Zhang Y K, Guo Y X and Li G F, Journal of Optoelectronics·Laser **26**, 250 (2016). (in Chinese)

[13] Zhou Y H, Zhao Z G, Li Y N, Zhang C S, Xie T, Cui Z G, Wang K, Tan X Y and Li C, Journal of Optoelectronics·Laser **26**, 422 (2015). (in Chinese)

[14] Chen Guo-hua, Liang Jun and Wang Xin-hua, Journal of South China University of Technology (Natural Science Edition) **41**, 142 (2013). (in Chinese)

[15] Kaphle M, Tan A C C, Thambiratnam D P and Chan T H T, Structural Control & Health Monitoring **19**, 187 (2012). (in Chinese)

[16] Wang W, Zeng Z and Yibo L I, Computer Engineering & Applications **49**, 230 (2013).

[17] Jin Z, Jiang M, Sui Q, Sai Y, Lu S, Cao Y, Zhang F and Jia L, Chinese Journal of Sensors & Actuators **26**, 1513 (2013).

[18] Huang X H, Zhang Y B, Tian B Z and Liu X X, Yantu Lixue/rock & Soil Mechanics **36**, 381 (2015).